Contents lists available at ScienceDirect

Solid State Ionics

Origin of enhanced catalytic activity of oxygen reduction reaction on zirconium oxynitrides: A first-principle study

Guangjin Wang[a,b,*], Fei Huang[c], Xiaobo Chen[d], Yi Yu[b,e], Chunli Gong[a], Hai Liu[a], Sheng Wen[a], Genwen Zheng[a], Mu Pan[b,*]

[a] College of Chemistry and Materials Science, Hubei Engineering University, Xiaogan 432000, China
[b] State Key Laboratory of Advanced Technology for Materials Synthesis and Processing, Wuhan University of Technology, Wuhan 430070, China
[c] Sericultural & Agri-Food Research Institute, Guangdong Academy of Agricultural Sciences, Key Laboratory of Functional Foods, Ministry of Agriculture, Guangdong Key Laboratory of Agricultural Products Processing, Guangzhou 510610, China
[d] Siyuan Laboratory, Guangzhou Key Laboratory of Vacuum Coating Technologies and New Energy Materials, Department of Physics, Jinan University, Guangzhou 510632, China
[e] Research & Advanced Technology Department, SAIC Motor, Shanghai 201804, China

ARTICLE INFO

ABSTRACT

To clarify the origin of the enhanced catalytic activity of zirconium oxynitrides, the first-principle calculation method is carried out to study the oxygen reduction reaction (ORR) on monoclinic ZrO_2 and cubic Zr_2ON_2 (011) surfaces. The relation of the d-orbital occupation of nonequivalence Zr atoms and the electron transfer between ORR intermediates and nonequivalence Zr atoms and the mechanism of ORR on the both (011) surfaces are investigated. The calculated results show that the d-orbital occupation of nonequivalence Zr atoms on cubic Zr_2ON_2 (011) surface is 32.60, which is higher than that on monoclinic ZrO_2 (011) surface (30.00). The mechanism of ORR on cubic Zr_2ON_2 (011) surface is a "dissociative mechanism", whereas that on monoclinic ZrO_2 (011) surface is an "associative mechanism". Compared to monoclinic ZrO_2 (011) surface, the enhanced catalytic activity of the ORR on cubic Zr_2ON_2 (011) surface is associated with the increase of electron transfer and the change of ORR mechanism, which is caused by the increase of the d-orbital occupation of its nonequivalence Zr atoms. Moreover, the Gibbs free energy calculated results show that the desorption process of OH^* on both (011) surfaces is the rate-limiting step of ORR.

1. Introduction

Owing to their merit of high-energy conversion efficiency and lower pollution, proton exchange membrane fuel cells (PEMFCs) have been considered as the most promising electrochemical devices [1]. Unfortunately, the practical application of PEMFCs is hindered by the high cost and insufficient of platinum (Pt), which is a well-known outstanding ORR catalyst [2]. For this reason, numerous efforts have been devoted to the development of alternative non-precious metal catalysts, such as pyrolyzing and non-pyrolyzing macrocyclic compounds, conductive polymers, transition metal chalcogenides/oxides/carbides/nitrides and so forth [3–6]. Among these promising catalysts, zirconia (ZrO_2) has attracted much attention due to its high chemical and electrochemical stability in an acidic media and oxidative atmospheres. However, the ORR catalytic activity of ZrO_2 is not satisfied with the requirements of commercial PEMFCs, since the onset potential of the ORR on ZrO_2/C is only 0.56 V [7], which is less than that of state-of-

the-art Pt/C catalysts [8]. As a result, many effective methods have been developed to improve the ORR catalytic activity of ZrO_2-based catalysts [7,9,10], in particular, the design and preparation of zirconium oxynitrides (ZrO_xN_y). For example, Zhang et al. [7] reported the ORR onset potential of ZrO_xN_y/C, which is prepared by using high temperature ammonolysis technologies, is 0.7 V in 0.5 M H_2SO_4 solution. Maekawa et al. [10] found that the ORR onset potential of ZrO_xN_y thin films which are synthesized via reactive sputtering method under O_2 and N_2 atmosphere is 0.8 V and that the thin films with the best ORR catalytic activity have a cubic Zr_2ON_2 crystalline structure. Nevertheless, they paid no attention to the origin of enhanced catalytic activity of the ORR on ZrO_xN_y. Solving this complicated problem is pivotal for design and preparation novel and high-efficiency transition metal oxynitride catalysts.

Density functional calculations are one of the most useful tools to solve these elusive problems [11,12]. Using molecular dynamics simulation method, Okamoto et al. [13] found that a spontaneous bond

---

breaking in HOOH on ZrO$_2$ (−111) surface suppresses the termination of the reaction at 2e$^-$ reduction. Their findings provide preliminary understanding of the ORR on ZrO$_2$ surface and pave the way for further exploring the ORR mechanism of ZrO$_2$. Based on the pioneering research by Okamoto et al., we studied the ORR on (−111), (−101) and (110) monoclinic ZrO$_2$ surfaces, as well as on (111) monoclinic surfaces, tetragonal and cubic phase ZrO$_2$ [14,15]. Our calculation results show that the catalytic activity of ORR on these selected surfaces increases with increasing their *d*-orbital occupation of nonequivalence Zr atoms. Although the relationship between ORR catalytic activity of ZrO$_2$ surfaces and their *d*-orbital occupation of nonequivalence Zr atoms is explored in our previous study, the effect of the increase of *d*-orbital occupation of nonequivalence Zr atoms on the electron transfer between ORR intermediates and nonequivalence Zr atoms and the mechanism of ORR on ZrO$_x$N$_y$ surfaces have not yet been realized. Solving these problems will give a clearer picture of the origin of enhanced catalytic activity of the ORR on ZrO$_x$N$_y$.

In this paper, using the first-principle calculation method, we investigated the ORR on monoclinic ZrO$_2$ and cubic Zr$_2$ON$_2$ (011) surfaces. Based on the relationship between the *d*-orbital occupation of nonequivalence Zr atoms on ZrO$_2$ surfaces and their catalytic activity for ORR [14,15], the *d*-orbital occupations of nonequivalence Zr atoms on monoclinic ZrO$_2$ and cubic Zr$_2$ON$_2$ (011) surfaces with and without adsorbed oxygen atoms were calculated. The mechanism of ORR on monoclinic ZrO$_2$ and cubic Zr$_2$ON$_2$ (011) surfaces was systematically studied. Moreover, Gibbs free energy diagrams were employed to estimate the energy barrier of ORR and identify the ORR rate-determining step on both chosen (011) surfaces.

2. Computational details

2.1. Calculation methods

The first-principle calculations were performed by using the Vienna Ab-initio Simulation Package (VASP) [16–18] with the Perdew-Burke-Ernzerh (PBE) parameterization of the generalized gradient approximation (GGA) adopted for the exchange correlation potential [19]. The projector augmented wave (PAW) method is used for dealing with the interaction between ions and electrons [20,21], and only $1s^1$, $2s^22p^3$, $2s^22p^4$ and $4d^25s^2$ were treated as valence electrons for H, N, O and Zr atoms, respectively. The energy cutoff for the plane wave basis was set to 500 eV. The force on each atom was lower than 0.02 eV Å^{-1}. All the geometry optimization was carried out with a conjugate gradient algorithm [22]. Spin-polarized density functional theory was adopted and the 4 × 4 × 1 and 8 × 8 × 1 Monkhorst-Pack *k* points were utilized for the geometry optimization and energy calculation of the chosen (011) surfaces, respectively [23]. The energy calculation of the chosen (011) surfaces was carried out with tetrahedron methods as corrected by Blöchl et al. [24]. Moreover, a Monkhorst-Pack scheme of 1 × 1 × 1 k points was utilized for geometry optimization and energy calculation of the isolate adsorbates [23]. The energy calculation of the isolate adsorbates was carried out with gaussian smearing functions [25], and the Gaussian smearing parameter was chosen to be σ = 0.1 eV. For understanding the charge transfer between the active atoms on chosen surfaces and their adsorbed ORR intermediates, a much more fine spacing between the grid points (180 × 180 × 180) and non-self-consistent calculation were carried out to perform bader charge analysis [26,27].

2.2. Computation models

To obtain the reasonable and stable surface of monoclinic ZrO$_2$ and cubic Zr$_2$ON$_2$, three rules (i.e. compactness condition, bond-breaking condition and electrostatic condition) were taken into account [28], when the (011) surface of monoclinic ZrO$_2$ and cubic Zr$_2$ON$_2$ were "carved" out of their corresponding relaxed bulk crystal. For keeping

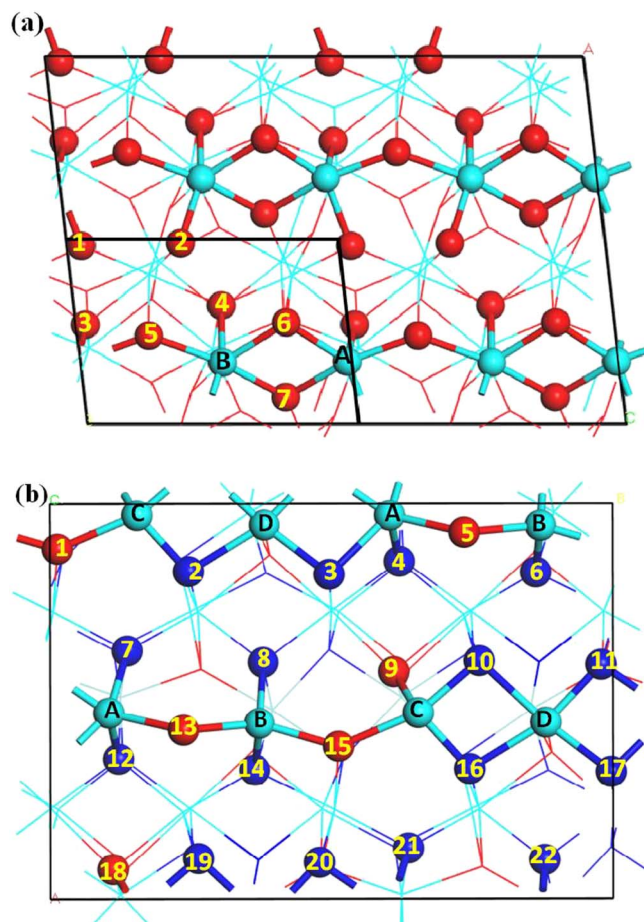**Fig. 1.** The top views of the (011) surface of monoclinic ZrO$_2$ (a) and cubic Zr$_2$ON$_2$ (b). The black square shows the quarter of monoclinic ZrO$_2$ (011) surface. The red, blue and bright green balls represent the oxygen, nitrogen and zirconium atoms, respectively. (For interpretation of the references to colour in this figure legend, the reader is referred to the web version of this article.)

constant the number of nonequivalence Zr atoms on the chosen surfaces, unit cells of (2 × 2) for monoclinic ZrO$_2$ and (1 × 1) for cubic Zr$_2$ON$_2$ were selected. The surface areas of the unit cells were 10.292 × 14.914 Å^2 for monoclinic ZrO$_2$ (011) and 10.180 × 14.364 Å^2 for cubic Zr$_2$ON$_2$ (011) surfaces, respectively. There were four Zr atomic layers in the both chosen (011) surfaces, and these layers repeated in three directions. In order to eliminate the interactions between two adjacent slabs, a vacuum layer of 12 Å was added into two successive slabs. The superficial of two Zr atomic layers of both (011) surfaces was allowed for unconstrained relaxation in three-dimension space, and the bottom two layers were fixed for simulating their corresponding bulk crystals.

3. Results and discussion

3.1. Stability of monoclinic ZrO$_2$ and cubic Zr$_2$ON$_2$ (011) surfaces

Fig. 1 shows the top view of the (011) surface of monoclinic ZrO$_2$ and cubic Zr$_2$ON$_2$. As shown in Fig. 1a that there are two nonequivalence Zr atoms and seven undercoordinated O atoms on the quarter of chosen surface (in the small black square) due to the symmetry of monoclinic ZrO$_2$ (011) surface. The nonequivalence Zr atoms are five-fold and six-fold coordinated, marking by letters A and B, respectively. The undercoordinated O atoms on the quarter of chosen surface are atoms 2 (two-fold coordinated, pointing outward from the surface), 5 and 6 (three-fold coordinated, pointing outward from the surface). Atoms 1 and 7 are three-fold coordinated (pointing downward